Original Article

The quantitative parameters derived from IDEAL-IQ in the lumbar vertebrae of healthy children: a pilot study of bone development

Jie Yang[1]^, Hui-Miao Sun[2]^, Hong Yang[2]^, Lei Hu[2]^, Jin-Liang Niu[3]^

[1]Department of Magnetic Resonance Imaging, The Affiliated Children's Hospital of Shanxi Medical University, Taiyuan, China; [2]Department of Magnetic Resonance Imaging, Children's Hospital of Shanxi, Women Health Center of Shanxi, Taiyuan, China; [3]Department of Magnetic Resonance Imaging, The Second Hospital of Shanxi Medical University, Taiyuan, China

Contributions: (I) Conception and design: J Yang, JL Niu, HM Sun; (II) Administrative support: HM Sun; (III) Provision of study materials or patients: J Yang, HM Sun; (IV) Collection and assembly of data: J Yang, H Yang, L Hu; (V) Data analysis and interpretation: J Yang, JL Niu; (VI) Manuscript writing: All authors; (VII) Final approval of manuscript: All authors.

Correspondence to: Jin-Liang Niu, PhD. Department of Magnetic Resonance Imaging, The Second Hospital of Shanxi Medical University, 382 Wuyi Road, Xinghualing District, Taiyuan 030001, China. Email: sxlscjy@163.com.

Background: Early childhood bone development affects that of bone disease in adolescence and adulthood. Many diseases can affect the cancellous bone or bone marrow. Therefore, it is of great significance to quantify the bone development of healthy children. The evaluation methods of bone development include bone age (BA) assessment and dual-energy X-ray bone mineral densitometry (DXA), both of which have strong subjectivity. The present study was conducted to improve our understanding of the bone development of healthy children using the quantitative parameters derived from iterative decomposition of water and fat with echo asymmetry and least squares estimation quantification (IDEAL-IQ) sequence.

Methods: Our study enrolled healthy children between January 2022 to December 2022 consecutively in Children's Hospital of Shanxi. The inclusion criteria were as follows: (I) age ≤18 years; (II) no contraindications (surgical and interventional devices for ferromagnetic materials, cardiac implantable electronic devices, cochlear implants, insulin pumps, dental implants containing metal or alloy) to magnetic resonance imaging (MRI) scan. The exclusion criteria were as follows: (I) previous malignant disease, (II) previous chemoradiotherapy, (III) previous spine surgery, (IV) previous or acute vertebral compression fracture, (V) artifacts present in images. Participants underwent MRI scans using IDEAL-IQ sequence in the lumbar vertebrae. The IDEAL-IQ parameters [proton density fat fraction (PDFF), 1/T2* (R2*)] were obtained. The factor analysis of variance was applied to compare the differences of PDFF and R2* in different lumbar vertebral groups. The Kruskal-Wallis *H* test or Mann-Whitney *U* test was applied to compare the differences of quantitative data among different gender or age groups. Spearman correlation analysis was applied to study the relationship among the age, PDFF, and R2*.

Results: A total of 145 participants (76 males, 69 females) were evaluated. There were no significant differences in PDFF and R2* of different lumbar vertebrae (P_{PDFF}=0.338, P_{R2*}=0.868). The average age was 36 [13–72] months. They were assigned into 4 groups (0–11, 12–35, 36–71, and 72–144 months). As the age increased, the average PDFF and R2* both increased significantly (r_{PDFF}=0.659, r_{R2*}=0.359, P<0.001). There were significant statistical differences in PDFF and R2* between the 4 age groups (Z_{PDFF}=46.651, Z_{R2*}=27.537, P<0.001). Moreover, the PDFF was also positively correlated with R2* (r=0.576, P<0.001). No association was found between the gender and PDFF, R2* (P_{PDFF}=0.949, P_{R2*}=0.177).

^ ORCID: Jie Yang, 0000-0002-6372-2655; Hui-Miao Sun, 0000-0003-2522-6607; Hong Yang, 0009-0001-6631-9706; Lei Hu, 0009-0002-5970-3598; Jin-Liang Niu, 0000-0002-4465-5477.

Conclusions: The quantitative parameters derived from IDEAL-IQ in the lumbar vertebrae of healthy children will improve our understanding of bone development and provide a basis for further exploring the diseases that affect children's bone development.

Keywords: Proton density fat fraction (PDFF); iterative decomposition of water and fat with echo asymmetry and least squares estimation quantification (IDEAL-IQ); magnetic resonance imaging (MRI); bone; development

Submitted May 18, 2023. Accepted for publication Oct 17, 2023. Published online Dec 04, 2023.
doi: 10.21037/qims-23-696
View this article at: https://dx.doi.org/10.21037/qims-23-696

Introduction

Bone development in childhood includes longitudinal growth and transverse growth for bone elongation and shaping, which changes dynamically with age. Whether the bone development is normal or not in early childhood affects the likelihood of bone disease in adolescence and adulthood (1,2). Furthermore, the trabecular bone and bone marrow change under pathological conditions (2). How to accurately judge the bone development of children and promote pediatric bone development should be comprehensively explored.

The evaluation methods of bone development in children include bone age (BA) assessment and dual-energy X-ray bone mineral densitometry (DXA). The BA evaluation methods (G&P mapping, TW scoring, China 05 method) are heavily subjective and the standard is difficult to master (3,4). DXA is unable to distinguish the quality differences between bone cortex and trabecular bone. A study found that the accuracy of DXA detection in infants under 3 years is not high (5). The evaluation methods of bone marrow development and diseases, such as bone aspiration and bone biopsy, are invasive. Although magnetic resonance imaging (MRI) is a non-invasive method, the performance of children's bone marrow in conventional T1-weighted imaging (T1WI) varies with age and location. Thus, the conventional MRI cannot accurately distinguish whether the bone development is normal or not.

The iterative decomposition of water and fat with echo asymmetry and least squares estimation quantification (IDEAL-IQ) technique provided a new approach for quantitative analysis of the cancellous bone and the fat content in bone marrow (6,7). Derived from mDIXON technology, IDEAL-IQ can generate a proton density fat fraction (PDFF) image, R2* image, fat image, water image, positive phase image, and reverse phase image during 1 scan. The scanning speed is fast, making it more suitable for children. The R2* refers to the reciprocal of T2* which reflects the cancellous bone content (7). A previous study revealed that PDFF was valuable in distinguishing aplastic anemia from myelodysplastic syndromes (8), and other studies have shown that the detection results of PDFF by MRI are highly consistent with the pathological results with good repeatability (9,10). Thus, IDEAL-IQ can simultaneously study the cancellous bone and the bone marrow development.

The component of bone in children changes with age, and many diseases can change the cancellous bone or the fat content of the bone. IDEAL-IQ can accurately evaluate PDFF and R2* of bone to study the bone development simultaneously. This study was conducted to quantify the fat and cancellous bone content of lumbar vertebrae in healthy children based on IDEAL-IQ, so as to quantify the normal bone development precisely and provide a basis for further studies focusing on diseases involving lumbar vertebrae. We present this article in accordance with the STROBE reporting checklist (available at https://qims.amegroups.com/article/view/10.21037/qims-23-696/rc).

Methods

Study participants

The study was conducted in accordance with the Declaration of Helsinki (as revised in 2013). This prospective cross-sectional study was approved by the local ethics committee of Children's Hospital of Shanxi (No. IRB-KYYN-2022-010) and written informed consent was provided by all participants' parents between January 2022 to December 2022. In our study, children who were suspected of having nervous system abnormality due to symptoms including enuresis, constipation, urinary retention, pyrexia, and weakness of the lower or all four extremities and underwent MRI of the lumbosacral spine

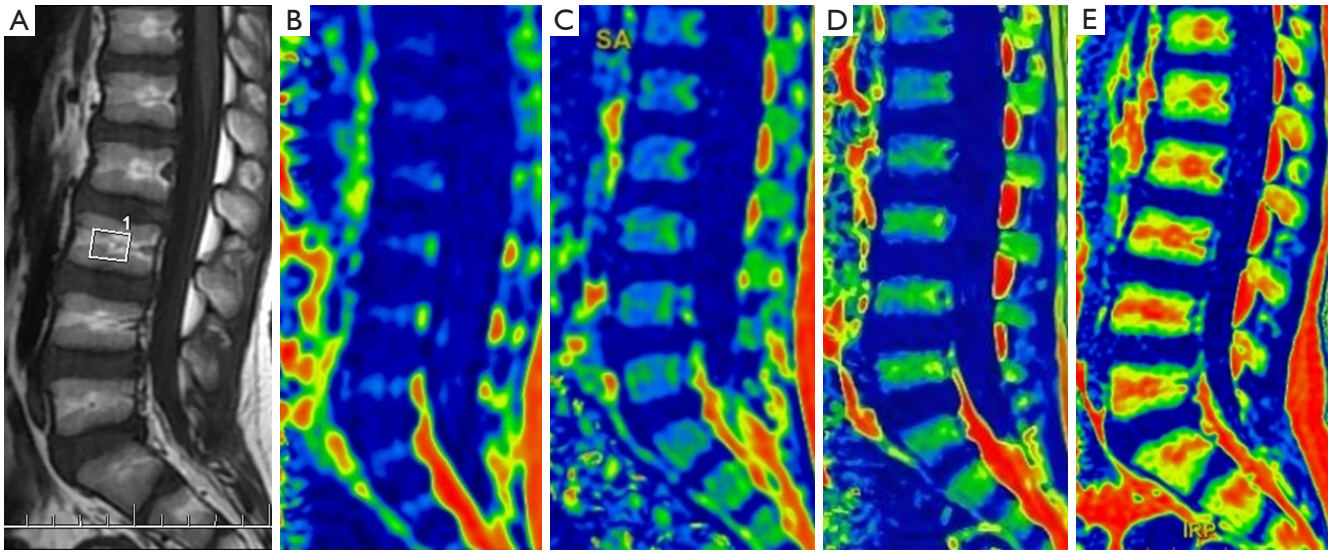

Figure 1 The PDFF figures of L1–5 vertebral body in different ages. (A) ROI; (B) 4 months; (C) 21 months; (D) 60 months; (E) 108 months. PDFF, proton density fat fraction; ROI, region of interest.

or the whole spine in Children's Hospital of Shanxi were enrolled, provided that they did not have any congenital abnormality in the whole spine or nervous system, metabolic disorders, blood system disorders, or trauma based on laboratory tests including hematology and urinalysis. The inclusion criteria were as follows: (I) age ≤18 years; (II) no contraindications (surgical and interventional devices for ferromagnetic materials, cardiac implantable electronic devices, cochlear implants, insulin pumps, dental implants containing metal or alloy) to MRI scan. The exclusion criteria were as follows: (I) previous malignant disease, (II) previous chemoradiotherapy, (III) previous spine surgery, (IV) previous or acute vertebral compression fracture, (V) artifacts present in images. Participants' ages and gender were collected.

MRI examination

MRI was performed on a 3.0-Tesla scanner (Discovery 750; GE Healthcare, Chicago, IL, USA) at the lumbar spine of all participants. All participants under 6 years of age underwent MRI examination after sedation by chloral hydrate. Participants were placed in the supine position. The MRI sequences consisted of sagittal T1WI and IDEAL-IQ. Parameters of sagittal T1WI were as follows: repetition time (TR) =400.0 ms; echo time (TE) =9.3 ms; slice thickness =3.0 mm; no gap; number of excitations (NEX) =4; field of view (FOV) =25 cm ×12.5 cm; matrix =320×192; acquisition time =2 min and 29 s. The IDEAL-IQ sequence scanning time was 1 min and 37 s; slice thickness =3 mm; layer spacing =0.3 mm; FOV =250 mm × 250 mm; matrix =256×228; echo train length =3; NEX =3.

IDEAL-IQ image analysis

All data of sagittal T1WI and IDEAL-IQ images were transferred to an Advantage Windows Workstation 4.7 (GE Healthcare) for processing. We used 3D SynchoView post-processing procedure for analyzing the PDFF and R2* maps. The regions of interests (ROIs) were placed at the center part of lumbar vertebral cancellous bone from L1 to L5 in order to minimize the effect of vertebral end-plate changes, vertebral venous plexus, and cerebrospinal fluid. We placed the ROIs on the T1WI image and cloned the same size and position of ROIs to the same places of the PDFF and R2* images, which allowed the values of PDFF and R2* to be obtained. ROIs placement on sagittal sections of the images were drawn by two readers independently (*Figure 1*). Another senior imaging physician judged the consistency of ROIs placement on sagittal sections between the two readers. Data for each participant were represented as the average of the two readers.

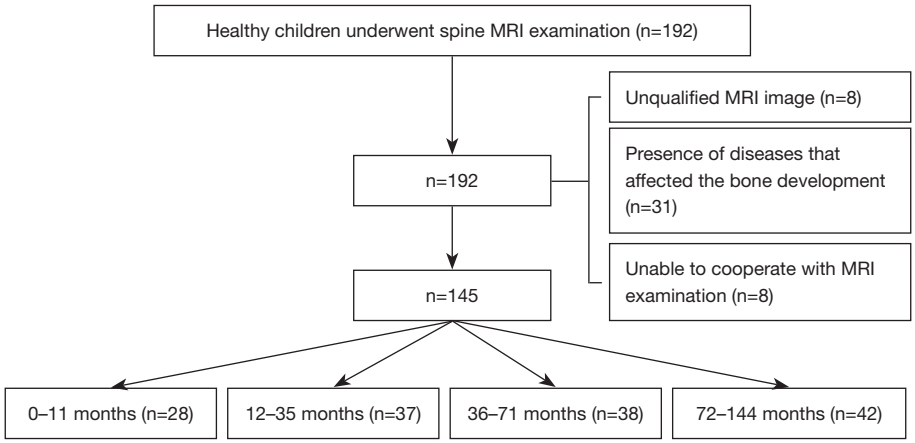

Figure 2 The flow chart of 145 healthy children. MRI, magnetic resonance imaging.

Table 1 Comparison of PDFF and R2* in different lumbar vertebral groups

Variables	L1 (n=145)	L2 (n=145)	L3 (n=145)	L4 (n=145)	L5 (n=145)	Z value	P value
PDFF	23.80 (15.88–33.24)	26.69 (18.00–34.90)	27.00 (16.80–36.50)	27.00 (18.12–38.40)	38.20 (29.85–46.48)	1.138	0.338
R2*	132.58 (116.60–156.70)	135.60 (114.25–165.82)	132.30 (112.82–157.85)	133.70 (114.69–158.75)	135.20 (114.77–157.99)	0.316	0.868

Factor analysis of variance. Data are presented as median (25–75% quantile). PDFF, proton density fat fraction; R2*, 1/T2*; L, lumbar.

Statistical analysis

Data analysis was performed by SPSS 25.0 (IBM Corp., Armonk, NY, USA). Quantitative data was expressed as median (25–75% quantile) whereas qualitative data was expressed by n (%). The factor analysis of variance (ANOVA) was applied to compare the differences of PDFF and R2* in different lumbar vertebral groups. The Kruskal-Wallis *H* test or Mann-Whitney *U* test was applied to compare the differences of quantitative data among different gender or age groups. Spearman correlation analysis was applied to study the relationship among the age, PDFF, and R2*.

Results

Participants

The final study sample consisted of 145 participants, among whom 76 children were males and 69 children were females. The age of the 145 healthy children was within 12 years. The average age was 36 [13–72] months. The flowchart shows initial number of study participants, participants excluded, and final study sample (*Figure 2*).

Comparison of PDFF and R2 in different lumbar vertebrae*

There were no significant differences were observed in PDFF and R2* in different lumbar vertebrae (P=0.338 and 0.868) (*Table 1*), so we used the average PDFF and the average R2* to analyze the statistical differences between different genders and age groups.

The relationship between gender and PDFF, R2 in the 145 children*

The average PDFF was 27.16 (16.43–36.03), and the average R2* was 134.62 (116.35–159.30). No association was found between the gender and PDFF (Z=0.063, P=0.949) or R2 * (Z=1.350, P=0.177) in the 145 children (*Table 2*).

*Spearman correlation analysis of the association between age and PDFF, R2**

Spearman correlation analysis was used to explore the

Table 2 The relationship between gender and PDFF, R2* in 145 children

Variables	Male (n=76)	Female (n=69)	Z value	P value
Average PDFF	27.88 (16.95–36.06)	27.06 (16.32–36.04)	0.063	0.949
Average R2*	131.36 (115.98–151.57)	139.36 (120.04–161.98)	1.350	0.177

Mann-Whitney *U* test. Data are presented as median (25–75% quantile). PDFF, proton density fat fraction; R2*, 1/T2*.

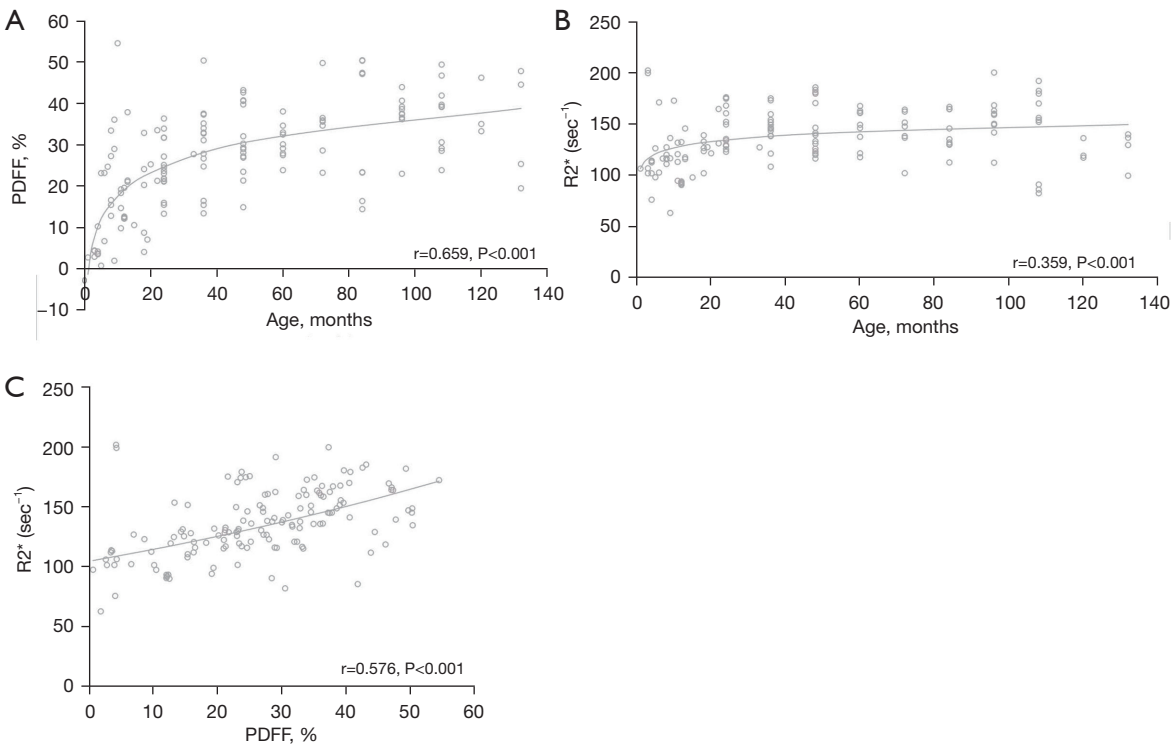

Figure 3 Scatter plots showing the correlation of PDFF with age (A), R2* with age (B), PDFF with R2* (C) values. PDFF, proton density fat fraction.

association among age, PDFF and R2*. Positive correlations were found between age and PDFF (r=0.659, P<0.001) and R2* (r=0.359, P<0.001). Moreover, it also indicated that the PDFF was positive correlated with R2* (r=0.576, P<0.001) (*Figure 3*).

Comparison of PDFF and R2 in different age groups*

The 145 healthy children were assigned into four age groups: 0–11 months group, 12–35 months group, 36–71 months group, and 72–144 months group. The average PDFF was 11.44 (3.74–23.09), 21.27 (12.45–26.12), 30.10 (26.75–35.60), and 37.37 (28.50–46.26); the average R2* was 114.50 (103.16–126.51), 128.38 (116.13–147.07), 145.34 (129.13–161.09), and 147.87 (129.21–163.58). As the age increased, the average PDFF (Z=46.651, P<0.001) and R2* (Z=27.537, P<0.001) both increased significantly (*Table 3*).

Discussion

In children, the bone development of the spine is the slowest and most diseases often involve the vertebrae, rendering it a commonly used site for study of normal bone development. We designed this study to quantify the cancellous bone and fat content of normal lumbar vertebrae of children at different ages. It was revealed that as the age increased, the average PDFF and R2* both increased significantly (P<0.001). Positive correlations were found

Table 3 Comparison of PDFF and R2* in different age groups

Variables	0–11 months (n=28)	12–35 months (n=37)	36–71 months (n=38)	72–144 months (n=42)	Z value	P value
Average PDFF	11.44 (3.74–23.09)	21.27 (12.45–26.12)	30.10 (26.75–35.60)	37.37 (28.50–46.26)	46.651	<0.001
Average R2*	114.50 (103.16–126.51)	128.38 (116.13–147.07)	145.34 (129.13–161.09)	147.87 (129.21–163.58)	27.537	<0.001

Kruskal-Wallis *H* test. Data are presented as median (25–75% quantile). PDFF, proton density fat fraction; R2*, 1/T2*.

among the different age groups (P<0.001). Moreover, the PDFF was also positively correlated with R2* (P<0.001).

PDFF is a new index reflecting the proportion of fat in bone marrow. Both osteoblasts and adipocytes in the marrow cavity originate from bone marrow mesenchymal cells (MSCs), and the differentiation of MSC into adipocytes and osteoblasts is affected by a variety of physiological and pathological factors (10-12). At the same time, various physiological and pathological changes of bone marrow are closely related to fat content. Therefore, the quantification of fat content in bone marrow is of great clinical significance for evaluating the impact of various physiological and pathological processes on spinal bone marrow and screening of disease-related information (13). When compared with yellow bone marrow, red bone marrow contains a lower fraction of fat and a higher fraction of water (10). Therefore, the PDFF in the bone marrow normally increases as childhood progress. A normal value of the PDFF for a 0–0.4-year-old is about 3%, whereas it is up to 32.9% for a 9–18-year-old (14). In our study, we found that as age increased, the average PDFF increased significantly (P<0.001). Then, the speed of conversion process from red bone marrow to yellow bone marrow decreased and the PDFF value gradually stabilized, which is consistent with a previous study (15). In addition, we found no association between gender and PDFF in healthy children, indicating that the bone marrow development between different genders was not statistically significantly different, which is consistent with a previous study (16). Several studies have also shown that the PDFF value was not associated with sex in adults (17,18).

R2* refers to the reciprocal of T2*. Quantitative MRI assessment of liver iron overload by means of R2* is a safe, non-invasive, and accurate alternative to liver biopsy (19). R2* calculations have also been used to assess iron-loading in other organs, such as the pancreas, spleen, and vertebral bone, in patients with anemia and primary hemochromatosis (20). Further, some studies have demonstrated that T2* values were negatively correlated with bone mineral density (BMD) (7,21,22). Therefore, we speculate that age also has an important impact on the R2* value. In our study, we found that as the age increased, the average R2* increased significantly (P<0.001). Finally, we found no association between gender and R2* in healthy children, indicating that the BMD and fat content of lumbar vertebrae between different genders were not statistically different. This has seldom been studied in previous studies in healthy children.

Regarding the relationship of PDFF and R2*, it was well known that bone marrow is present in the trabecular bone (10). With the increase of children's age and height, all kinds of bone tissues increase. Bone marrow cavities gradually expand with osteogenesis activity, osteoclast activity, and trabecular bone reconstruction. Components of the bone marrow, such as adipose tissue, also increase to provide the nutrition for bone growth. Moreover, the R2* of fat is larger than that of water (23), so the increase in fat proportion may lead to an increase in the total R2* of the vertebral body. We believe that PDFF is associated with R2*, and our present study precisely confirms this point. We will further investigate the mechanism of PDFF and R2* correlation in the future.

Limitations

Due to ethical limitations, we could not obtain pathological specimens of lumbar vertebrae from healthy children. Moreover, the participants of our study only included infants, toddlers, preschool children and school children, not teenagers. We will recruit teenagers in the follow-up study.

Conclusions

As the age increased, the average PDFF and R2* of lumbar vertebrae both increased significantly in healthy children. These findings will probably improve our understanding of the bone development and enable differential diagnosis other diseases of children's bone. In our next research, we will explore the microstructural changes in the skeletal tissue of children with leukemia.

Acknowledgments

Funding: None.

Footnote

Reporting Checklist: The authors have completed the STROBE reporting checklist. Available at https://qims.amegroups.com/article/view/10.21037/qims-23-696/rc

Conflicts of Interest: All authors have completed the ICMJE uniform disclosure form (available at https://qims.amegroups.com/article/view/10.21037/qims-23-696/coif). The authors have no conflicts of interest to declare.

Ethical Statement: The authors are accountable for all aspects of the work in ensuring that questions related to the accuracy or integrity of any part of the work are appropriately investigated and resolved. The study was conducted in accordance with the Declaration of Helsinki (as revised in 2013). This study was approved by the local ethics committee of Children's Hospital of Shanxi (No. IRB-KYYN-2022-010) and written informed consent was provided by all participants' parents.

References

1. Land C, Schoenau E. Fetal and postnatal bone development: reviewing the role of mechanical stimuli and nutrition. Best Pract Res Clin Endocrinol Metab 2008;22:107-18.
2. Rosen CJ, Ackert-Bicknell C, Rodriguez JP, Pino AM. Marrow fat and the bone microenvironment: developmental, functional, and pathological implications. Crit Rev Eukaryot Gene Expr 2009;19:109-24.
3. Berst MJ, Dolan L, Bogdanowicz MM, Stevens MA, Chow S, Brandser EA. Effect of knowledge of chronologic age on the variability of pediatric bone age determined using the Greulich and Pyle standards. AJR Am J Roentgenol 2001;176:507-10.
4. Zhang SY. Bone age standard of Chinese wrist: China 05 and its application. Beijing: Science and Technology Press, 2015.
5. Kopiczko A, Adamczyk JG, Łopuszańska-Dawid M. Bone Mineral Density in Adolescent Boys: Cross-Sectional Observational Study. Int J Environ Res Public Health 2020;18:245.
6. Li X, Lu R, Xie Y, Li Q, Tao H, Chen S. Identification of abnormal BMD and osteoporosis in postmenopausal women with T2*-corrected Q-Dixon and reduced-FOV IVIM: correlation with QCT. Eur Radiol 2022;32:4707-17.
7. Yun JS, Lee HD, Kwack KS, Park S. Use of proton density fat fraction MRI to predict the radiographic progression of osteoporotic vertebral compression fracture. Eur Radiol 2021;31:3582-9.
8. Samet JD, Deng J, Schafernak K, Arva NC, Lin X, Peevey J, Fayad LM. Quantitative magnetic resonance imaging for determining bone marrow fat fraction at 1.5 T and 3.0 T: a technique to noninvasively assess cellularity and potential malignancy of the bone marrow. Pediatr Radiol 2021;51:94-102.
9. Schmeel FC, Vomweg T, Träber F, Gerhards A, Enkirch SJ, Faron A, Sprinkart AM, Schmeel LC, Luetkens JA, Thomas D, Kukuk GM. Proton density fat fraction MRI of vertebral bone marrow: Accuracy, repeatability, and reproducibility among readers, field strengths, and imaging platforms. J Magn Reson Imaging 2019;50:1762-72.
10. Yu L, Xie M, Zhang F, Wan C, Yao X. TM9SF4 is a novel regulator in lineage commitment of bone marrow mesenchymal stem cells to either osteoblasts or adipocytes. Stem Cell Res Ther 2021;12:573.
11. Wang C, Meng H, Wang X, Zhao C, Peng J, Wang Y. Differentiation of Bone Marrow Mesenchymal Stem Cells in Osteoblasts and Adipocytes and its Role in Treatment of Osteoporosis. Med Sci Monit 2016;22:226-33.
12. Rinker TE, Hammoudi TM, Kemp ML, Lu H, Temenoff JS. Interactions between mesenchymal stem cells, adipocytes, and osteoblasts in a 3D tri-culture model of hyperglycemic conditions in the bone marrow microenvironment. Integr Biol (Camb) 2014;6:324-37.
13. Zeng Z, Ma X, Guo Y, Ye B, Xu M, Wang W. Quantifying Bone Marrow Fat Fraction and Iron by MRI for Distinguishing Aplastic Anemia from Myelodysplastic Syndromes. J Magn Reson Imaging 2021;54:1754-60.
14. Ruschke S, Pokorney A, Baum T, Eggers H, Miller JH, Hu HH, Karampinos DC. Measurement of vertebral

bone marrow proton density fat fraction in children using quantitative water-fat MRI. MAGMA 2017;30:449-60.
15. Yoo HJ, Hong SH, Kim DH, Choi JY, Chae HD, Jeong BM, Ahn JM, Kang HS. Measurement of fat content in vertebral marrow using a modified dixon sequence to differentiate benign from malignant processes. J Magn Reson Imaging 2017;45:1534-44.
16. Kühn JP, Hernando D, Meffert PJ, Reeder S, Hosten N, Laqua R, Steveling A, Ender S, Schröder H, Pillich DT. Proton-density fat fraction and simultaneous R2* estimation as an MRI tool for assessment of osteoporosis. Eur Radiol 2013;23:3432-9.
17. Colombo A, Bombelli L, Summers PE, Saia G, Zugni F, Marvaso G, Grimm R, Jereczek-Fossa BA, Padhani AR, Petralia G. Effects of Sex and Age on Fat Fraction, Diffusion-Weighted Image Signal Intensity and Apparent Diffusion Coefficient in the Bone Marrow of Asymptomatic Individuals: A Cross-Sectional Whole-Body MRI Study. Diagnostics (Basel) 2021.
18. Ning Q, Fan T, Tang J, Han S, Wang W, Ren H, Wang H, Ye H. Preliminary analysis of interaction of the fat fraction in the sacroiliac joint among sex, age, and body mass index in a normal Chinese population. J Int Med Res 2020;48:300060520931281.
19. França M, Martí-Bonmatí L, Porto G, Silva S, Guimarães S, Alberich-Bayarri Á, Vizcaíno JR, Pessegueiro Miranda H. Tissue iron quantification in chronic liver diseases using MRI shows a relationship between iron accumulation in liver, spleen, and bone marrow. Clin Radiol 2018;73:215.e1-9.
20. Kwack KS, Lee HD, Jeon SW, Lee HY, Park S. Comparison of proton density fat fraction, simultaneous R2*, and apparent diffusion coefficient for assessment of focal vertebral bone marrow lesions. Clin Radiol 2020;75:123-30.
21. Papakonstantinou O, Alexopoulou E, Economopoulos N, Benekos O, Kattamis A, Kostaridou S, Ladis V, Efstathopoulos E, Gouliamos A, Kelekis NL. Assessment of iron distribution between liver, spleen, pancreas, bone marrow, and myocardium by means of R2 relaxometry with MRI in patients with beta-thalassemia major. J Magn Reson Imaging 2009;29:853-9.
22. Kim D, Kim SK, Lee SJ, Choo HJ, Park JW, Kim KY. Simultaneous Estimation of the Fat Fraction and $R_2(*)$ Via $T_2(*)$-Corrected 6-Echo Dixon Volumetric Interpolated Breath-hold Examination Imaging for Osteopenia and Osteoporosis Detection: Correlations with Sex, Age, and Menopause. Korean J Radiol 2019;20:916-30.
23. Hopkins JA, Wehrli FW. Magnetic susceptibility measurement of insoluble solids by NMR: magnetic susceptibility of bone. Magn Reson Med 1997;37:494-500.

Cite this article as: Yang J, Sun HM, Yang H, Hu L, Niu JL. The quantitative parameters derived from IDEAL-IQ in the lumbar vertebrae of healthy children: a pilot study of bone development. Quant Imaging Med Surg 2024;14(1):136-143. doi: 10.21037/qims-23-696

